Magn Reson Med Sci 2020; 19; 14–20
doi:10.2463/mrms.mp.2018-0097
Published Online: April 5, 2019

MAJOR PAPER

Statistical Analysis of the Apparent Diffusion Coefficient in Patients with Clinically Mild Encephalitis/Encephalopathy with a Reversible Splenial Lesion Indicates That the Pathology Extends Well beyond the Visible Lesions

Yang Qing[1], Wang Xiong[2], Huang Da-xiang[3], Zhu Juan[1], Wang Fei[1], and Yu Yong-qiang[4*]

Purpose: To investigate whether the genu of the corpus callosum is involved in patients with clinically mild encephalitis/encephalopathy with a reversible splenial lesion (MERS) type I.

Methods: Twenty-three cases of clinically confirmed MERS I were analyzed retrospectively, and MRI features of the lesion were observed. The apparent diffusion coefficient (ADC) values of the same region of interests in lesions at the splenium and genu of the corpus callosum were measured before and after treatment (i.e., four groups), and the average ADC values were calculated. Paired *t*-tests were used to compare the ADC values of lesions in the splenium and genu before and after treatment. Independent sample *t*-tests were used to compare the values in the splenium and genu after treatment.

Results: The mean ADC values of the splenium before and after treatment were 0.448 ± 0.124 and 0.790 ± 0.070 × 10^{-3} mm^2/s, respectively, showing significant difference ($P < 0.01$). The mean ADC values in the genu before and after treatment were 0.783 ± 0.067 and 0.829 ± 0.070 × 10^{-3} mm^2/s, respectively, also showing significant difference ($P < 0.01$). There was no significant difference in the ADC values between the splenium and genu after treatment ($P > 0.05$).

Conclusion: The genu showed a slight restriction in diffusion in the acute stage of type I MERS. After treatment, this diffusion restriction diminished as it typically does in the splenium. Our results indicate that the pathology in MERS extends well beyond the visible lesions.

Keywords: *apparent diffusion coefficient value, corpus callosum, magnetic resonance imaging, clinically mild encephalitis/encephalopathy with reversible splenial lesion*

Introduction

Clinically mild encephalitis/encephalopathy with a reversible splenial lesion (MERS) is a clinico-radiological syndrome first reported by Tada et al.,[1] and subsequently further described by Takanashi et al.,[2] and Garcia-Monco et al.[3] described the clinical imaging syndrome in detail and proposed a new name, "reversible splenial lesion syndrome (RESLES)". The cause of and mechanism underlying this disease are not completely clear. In most cases, the clinical and imaging abnormalities of MERS are reversible. However, in some cases (such as in patients with severe hypoglycemia), if it is not treated in time, marked central nervous system damage may occur; therefore, Starkey et al.[4] suggested that the syndrome be named as "cytotoxic lesions of the corpus callosum," to highlight the partial irreversibility of the disease. Takanashi et al.[5] proposed dividing MERS into two types based on the extent of the lesion: type I lesions are limited to the splenium of the corpus callosum (SCC) on MR images, while type II lesions spread to the entire corpus callosum, adjacent white matter or both. They further speculated that type I had undergone a type II process, or that other parts of the corpus callosum (i.e., the body and the genu) and adjacent white matter were only slightly involved and could not be seen in routine diffusion-weighted imaging (DWI). This hypothesis has not been confirmed by experiments. However, understanding the actual

[1]Department of MRI, Anqing Municipal Hospital, Anhui, China
[2]Department of Neurology, Anqing Municipal Hospital, Anhui, China
[3]Department of Endocrinology, Anqing Municipal Hospital, Anhui, China
[4]The First Affiliated Hospital of Anhui Medical University, 81 Meishan Road, Hefei, Anhui 230032, China
*Corresponding author, E-mail: yongqiang_yu@sohu.com

Received: August 6, 2018 | Accepted: January 26, 2019

extent of MERS is an important step toward understanding the pathology of this disease.

The purpose of this study is to verify or disprove Takanashi et al.'s hypothesis[5] about the range of MERS lesions. We thus performed a retrospective review of the medical and MRI records of 23 patients identified as having "MERS type I" or "RESLES type I." The mean apparent diffusion coefficient (ADC) values of the SCC and genu of the corpus callosum (GCC) before and after treatment were quantitatively measured and compared.

Materials and Methods

Patients

This study was approved by the Institutional Review Board before initiation (Decision No. 2017-01-001). The requirement for informed consent was waived because of the retrospective study design.

Twenty-three patients with MERS type I were identified in a tertiary referral hospital from January 2012 to November 2017 using a radiological database and their clinical and radiologic data were reviewed. These patients included 8 males and 15 females, with age at diagnosis ranging from 2 to 63 years, mean age: 16 ± 8.0 years. Eleven cases (47.83%) involved children. These 23 patients were diagnosed with MERS type I, based on the following criteria as set forth by Garcia-Monco et al.[3]: 1) neurological symptoms and signs such as headache, weakness of the limbs, aphasia, loss of consciousness, etc.; 2) MRI images showing cytotoxic edema in typical locations (lesions limited to the SCC); 3) both the imaging findings and clinical symptoms were reversible with treatment.

MRI equipment and scanning parameters

For MRI, we used a 3T superconducting magnetic resonance system (Discovery MR750, General Electric Healthcare, Milwaukee, IL, USA) and a standard 8-channel head coil. The sequences and parameters were: transverse T_1WI-fluid-attenuated inversion recovery (FLAIR); transverse and sagittal T_2WI-periodically rotated overlapping parallel lines with enhanced reconstruction (PROPELLER); transverse DWI (echo-planar imaging sequence, *b*-value set as 0, 1000 s/mm^2; TR = 3000 ms, TE = 97 ms, FOV, 240 × 240 mm; matrix = 160 × 160, slice thickness = 5.5 mm; intersection gap = 1.5 mm; number of excitations = 2), and ADC-Map. The automatic head scan software-READY Brain (General Electric) was used in the follow-up MR scanning process to avoid layer interleaving. The interval between the appearance of clinical symptoms and the first MRI examination was 1–11 days, with an average of 3.9 days. The interval between the first MRI examination and the first follow-up was 5–29 days, with an average of 10.3 days.

Image processing and analysis

Two radiologists, each with more than 5 years of experience, confirmed the anatomical locations of the lesions and the abnormal signal intensities on T_1WI, T_2-WI, DWI, and ADC-map scans by cross-checking on an AW4.6 workstation (General Electric Healthcare). The ADC values were measured using Functool-ADC software (General Electric Healthcare). ROIs were automatically generated by the Functool-ADC software (round shape, 58 mm^2), and the ROIs were carefully copied and placed in the center of the GCC and SCC (Fig. 1); this was jointly confirmed by two radiologists. To avoid layer interleaving during the follow-up examination, we used the automatic head-scan software READY Brain (General Electric Healthcare), in follow-up MR scans. Four groups of ADC values were measured and recorded: SCC in the initial examination (group 1), SCC in the first follow-up examination after treatment (group 2), GCC in the initial examination (group 3), and GCC in the first follow-up examination after treatment (group 4); each of the ROIs' ADC values were measured by two radiologists, independently. If the data obtained from the same ROI by each radiologist differed, the average value was used for the statistical analysis.

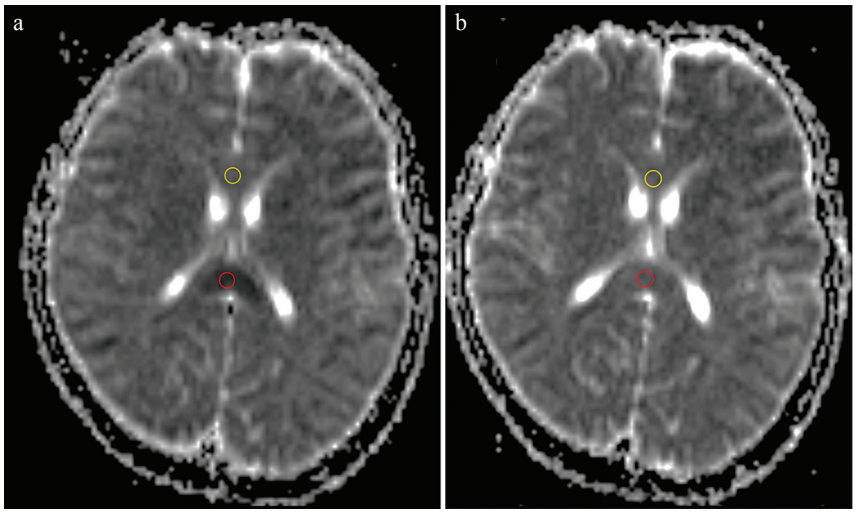

Fig. 1 A round ROI (58 mm^2) is automatically generated by Functool-ADC software (General Electric Healthcare, Milwaukee, IL, USA). The ROI is carefully copied and placed in the center of the genu and splenium of the corpus callosum. The location of the ROIs was jointly confirmed by two radiologists. (**a**) The location of ROIs in the initial examination. (**b**) The location of ROIs in the follow-up examination. ADC, apparent diffusion coefficient.

Statistical analysis

The four groups of ADC values were statistically analyzed using IBM SPSS Statistics, version 19.0 (IBM Corporation, Armonk, NY, USA). Data conforming to a normal distribution are expressed as mean ± standard deviation. Paired *t*-tests were used to compare the means of groups 1 and 2, and of groups 3 and 4. Independent sample *t*-tests were used to compare the means of groups 2 and 4. Results with $P < 0.05$ were considered statistically significant. Statistical results are given to an accuracy of three decimal places.

Results

The clinical data and radiological images of 23 patients were reviewed by all authors together. The basic information and clinical findings of the patients are summarized in Tables 1 and 2. One of the patients with diabetes who also showed hyperthyroidism, was counted once for statistical analysis. Six patients (26.08%) developed hyponatremia (mean serum sodium value: 131.7 ± 4.1 mmol/L; normal range, 135–145 mmol/L) during the course of their disease, but no patient developed hypokalemia. One patient showed severe hyponatremia (serum sodium: 123 mmol/L).

In the initial MRI examination, a total of 23 lesions were found in 23 MERS type I patients. The morphology and MR features of the lesions are summarized in Table 3. Based on the morphology, lesions of the SCC in MERS type I patients could be categorized into three forms: circle-shaped (seven cases, 30.43%, Fig. 2a), oval-shaped (13 cases, 56.52%, Fig. 2b), and boomerang-shaped (three cases, 13.04%, Fig. 2c). DWI showed augmented signals (23 cases, 100%), and the ADC-map showed diminished signals (23 cases, 100%). The 23 lesions had disappeared completely (100%) by the follow-up MR examination.

For the 23 MERS type I cases, the mean ADC value, the standard deviation, the *P*-value and the results of paired

Table 1 Basic information for 23 patients included in this study

Patient No.	Age (years)	Sex	Cause of MERS	Days from symptom onset to initial MR examination	Days from follow-up to initial MR examination	Type of MERS	Shape of MERS in SCC
1	2	Female	Viral encephalitis	4	11	I	Olivary
2	2	Female	Viral encephalitis	4	10	I	Boomerang
3	4	Female	Viral encephalitis	3	10	I	Circle
4	4	Female	Viral encephalitis	4	7	I	Olivary
5	8	Female	Mycoplasmal encephalitis	3	10	I	Boomerang
6	9	Female	Viral encephalitis	6	8	I	Boomerang
7	10	Male	Viral meningoencephalitis	7	10	I	Olivary
8	11	Female	Viral encephalitis	3	7	I	Olivary
9	13	Male	Central nervous system infection	3	5	I	Olivary
10	15	Male	Viral meningitis	2	11	I	Circle
11	17	Female	Central nervous system infection	5	7	I	Circle
12	21	Male	Thyroid storm	6	12	I	Olivary
13	23	Female	Eclampsia (Iatrogenic drugs)	1	11	I	Olivary
14	23	Male	Viral encephalitis	5	10	I	Circle
15	23	Male	Tuberculosis hemoptysis (Iatrogenic drugs)	5	7	I	Circle
16	24	Female	Viral encephalitis	3	8	I	Circle
17	26	Female	Brain injury	1	29	I	Olivary
18	27	Male	Hemorrhagic fever with renal syndrome	3	11	I	Olivary
19	35	Male	Viral encephalitis	2	8	I	Olivary
20	44	Female	Central nervous system infection	11	12	I	Olivary
21	44	Female	Viral encephalitis	3	15	I	Olivary
22	55	Female	Hypoglycemia	4	7	I	Olivary
23	63	Female	Diabetes complicated with chronic renal insufficiency	1	11	I	Circle

MERS: mild encephalitis/encephalopathy with a reversible splenial lesion; SCC: splenium of the corpus callosum.

Table 2 Clinical data of patients with clinically mild encephalitis/encephalopathy with a reversible splenial lesion (MERS)

Etiologic group and serum sodium	No. of patients (%)	Treatment	Clinical outcomes
Infectious disease	17 (73.91)	Anti-virus, anti-infection, symptomatic treatment	CR
Central nervous system infection	16 (69.57)	Anti-virus, Anti-infection, symptomatic treatment	CR
Systemic infection (hemorrhagic fever with renal syndrome)	1 (4.35)	Anti-virus, symptomatic treatment	CR
Metabolic-related diseases (diabetes, hypoglycemia, etc.)	3 (13.04)	Correct electrolyte and blood sugar	CR
Acute craniocerebral injury	1 (4.35)	Epidural hematoma removal, symptomatic treatment	CR
Iatrogenic drugs	2 (8.70)	Suspend use of drug	CR
Hyponatremia	6 (26.09)	Correct electrolyte	CR

CR, complete recovery.

Table 3 Lesion classification and morphology in the initial MR image of 23 cases of clinically mild encephalitis/encephalopathy with a reversible splenial lesion (MERS)

Itemize	DWI	ADC-map	Lesion shape		
MR feature	High	Low	Circle	Olivary	Boomerang
Number of cases	23	23	7	13	3
Ratio (%)	100.0	100.0	30.43	56.52	13.04

DWI, diffusion-weighted imaging; ADC, apparent diffusion coefficient.

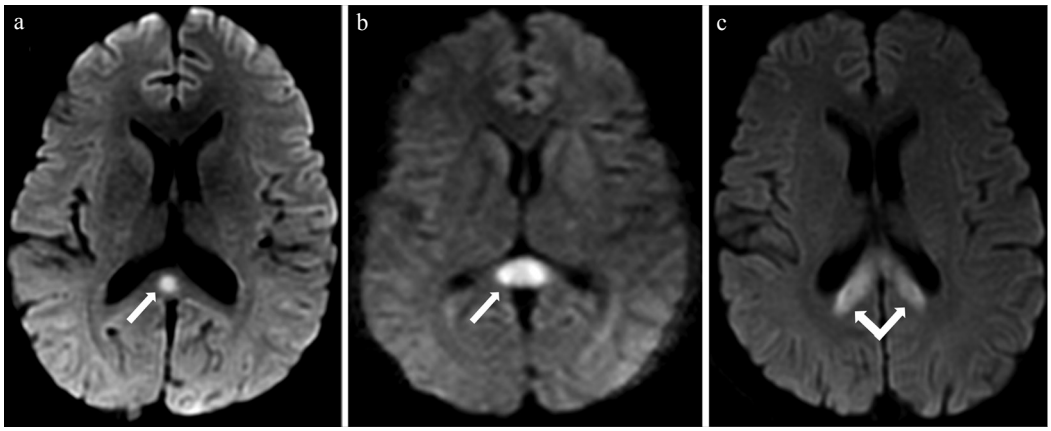

Fig. 2 Shape of SCC lesions in MERS type I; (**a**) circle shape, (**b**) oval shape, (**c**) boomerang shape. There is no visible reduced diffusion in the genu. SCC, splenium of the corpus callosum; MERS, mild encephalitis/encephalopathy with a reversible splenial.

t-tests for the same ROIs in the SCC and GCC before and after treatment are shown in Table 4. The ADC values of the SCC before and after treatment differed as statistically significant ($t = -12.157$, $P = 3.096 \times 10^{-11}$). The ADC values of the GCC before and after treatment were also differed as statistically significant ($t = -4.780$, $P = 9.000 \times 10^{-5}$). ADC values in the SCC and GCC after treatment did not differ statistically significant ($t = -1.907$, $P = 0.063$). Figure 3 shows a box plot for a visual comparison of the median, four quartiles, and extreme values (maximum and minimum values) of the four sets of data.

Discussion

In this study, we found that in the acute phase, the SCC showed high-intensity lesions that were typically symmetrical without enhancement on T_2 and diffusion-weighted sequences. The lesions showed ADC value reduction on ADC-maps.

In general, MERS lesions showed cytotoxic edema in typical anatomical locations, and the lesions usually disappeared from the MRI scans within a week or a few weeks (Table 1 and Fig. 4). There has been at least one report of lesions not disappearing for months,[6] but we did not encounter such delayed disappearance in this study.

The mean ADC value of lesions in the SCC before treatment was $0.448 \pm 0.124 \times 10^{-3}$ mm^2/s. After treatment, the mean ADC value of lesions in the SCC was increased to $0.790 \pm 0.070 \times 10^{-3}$ mm^2/s (Table 4). These changes in ADC values of lesions in the SCC of MERS patients after treatment were statistically significant. Dardzinski et al.[7] argued that lesions may be reversible when the ADC value of the lesion is $0.450–0.550 \times 10^{-3}$ mm^2/s, but if the value was

Table 4 Mean ADC value and results of paired samples *t*-test on the same region of interest in the SCC and GCC before and after the treatment of 23 cases of clinically mild encephalitis/encephalopathy with a reversible splenial lesion (MERS)

Location	The initial examination (10^{-3} mm^2/s)	Follow-up examination (10^{-3} mm^2/s)	*t*	*P*
SCC	0.448 ± 0.124	0.790 ± 0.070	−12.157	3.096×10^{-11}
GCC	0.783 ± 0.067	0.829 ± 0.070	−4.780	9.000×10^{-5}

Results are shown as mean ± standard deviation. ADC, apparent diffusion coefficient; SCC, splenium of the corpus callosum; GCC, genu of the corpus callosum.

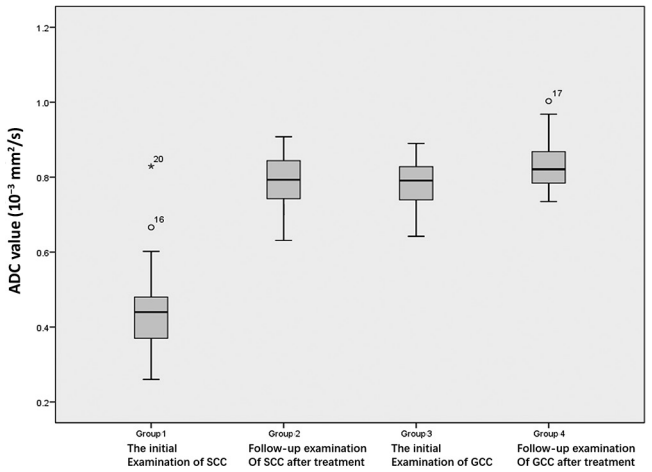

Fig. 3 SPSS box plots showing the median, four quantiles, maximum, and minimum ADC values from 92 regions of interest (23 MERS type I patients) for four sets of data: initial examination of SCC (group 1, 23 ROIs); follow-up examination of SCC after treatment (group 2, 23 ROIs); initial examination of GCC (group 3, 23 ROIs); follow-up examination of GCC after treatment (group 4, 23 ROIs). Numbers in the box plots indicated the patient No. (corresponding to Table 1). ADC, apparent diffusion coefficient; SCC, splenium of the corpus callosum; GCC, genu of the corpus callosum; asterisk, the extreme value of the data group; circle, the outlier value of the data group; MERS, mild encephalitis/encephalopathy with a reversible splenial.

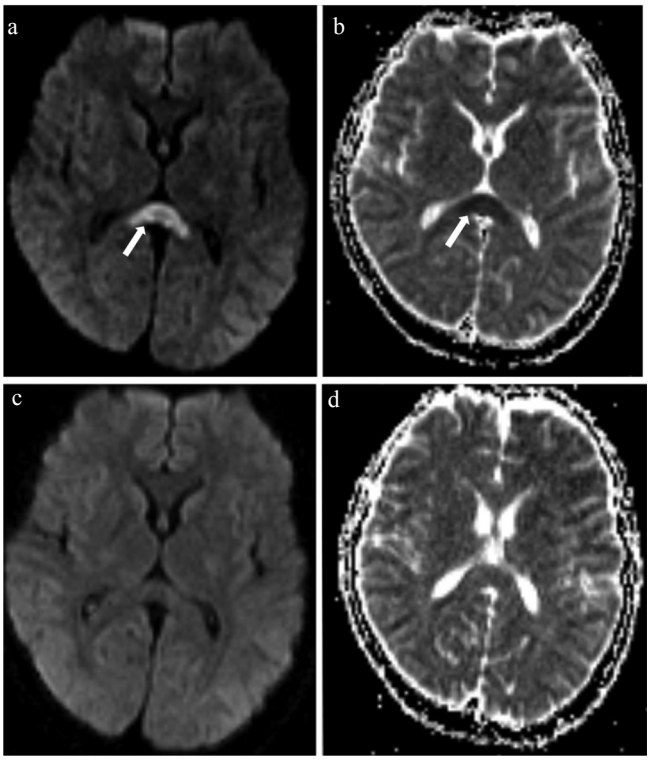

Fig. 4 Magnetic resonance images from a 23-year-old man presenting with headache. (**a** and **b**) Axial DWI and ADC map showing reduced diffusion in the splenium (arrows), which is a typical MERS type I presentation. There is no visible reduced diffusion in the genu. (**c** and **d**) Follow-up axial DWI and ADC map after 10 days of symptomatic treatment, showing that the lesions had disappeared. DWI: diffusion-weighted imaging; ADC: apparent diffusion coefficient; MERS, mild encephalitis/encephalopathy with a reversible splenial.

lower than this threshold, the lesion was not reversible. In our study, all lesions in the 23 MERS patients were reversed by treatment. Even, a lesion with an ADC value of 0.260×10^{-3} mm^2/s, occurring in one patient, was still reversible. Thus, when using the ADC value to judge the prognosis of MERS, it is necessary to consider that different pathological mechanisms may yield different results.

The extreme (maximum) values (patient No. 20) in the box plots (Fig. 3, star symbol) were obtained in the initial MRI examinations on day 11 after the appearance of clinical symptoms (corresponding to Table 1, patient No. 20). As previously reported in the literature, SCC signal abnormalities may reduce most rapidly within 2 days of the initial MR examination.[3] This patient (No. 20) may therefore have been in the recovery period, so that diffusion was restricted in the shrinking lesions (yielding a high ADC value).

It should be noted that the patients included in this study were diagnosed with MERS type I (100%). Although the lesions in type I MERS were diverse (Table 3 and Fig. 2), none of the lesions on conventional MR (including DWI and ADC-map) images were found outside the SCC region. However, if Takanashi et al.'s[5] speculations are correct, a statistical analysis of the ADC values of the GCC should make it possible to detect the same ADC value changes that are seen in the SCC (albeit mild). Quantitative measurements and statistical analyses in this study found that in the acute stage of MERS, not only the SCC, but also the GCC region showed mild diffusion restriction (an ADC value decrease), which is not easy to detect. GCC diffusion restriction showed a recovery, as it does in the SCC after a period of time (Table 4). In previous studies,[5,8] diffusion restriction was not detected in the GCC in patients with MERS type I, probably

because the signal changes were minor and not easily detected by human eyes.

Clinically, the syndrome is associated with a wide spectrum of conditions. The neurological symptoms of MERS usually resolve completely, without neurological sequelae after a short disease course.[3] However, the underlying pathophysiological mechanism of MERS remains unclear. Takanashi et al.[5] proposed that the type I lesions are limited to the SCC on MR images, while type II lesions spread to the entire corpus callosum, adjacent white matter or both. They further speculated that MERS type II resolved completely by passing through a MERS type I stage exhibiting an isolated splenial lesion, or that other parts of the corpus callosum and adjacent white matter were only minimally involved and changes in these regions could not be detected by routine DWI. Our research adds evidence supporting this speculation. Lin et al.[9] reported the case of a 36-year-old male patient with MERS type I, with *Staphylococcus aureus* meningitis, whose NAA/Cr, NAA/Cho, and Cho/Cr ratios were abnormal in all examined regions of the brain, suggesting that the pathological changes in MERS actually involve the entire brain. Tsubouchi et al.[10] reported that the range of lesions in high *b*-value (*b* = 3000) DWI was larger than that seen with conventional *b*-value (*b* = 1000) DWI (six cases), and in one case, lesions were observed within a high *b* value (*b* = 3000) that could not be seen with conventional *b* values (*b* = 1000). They did not statistically analyze their results. However, taking these results together with those of our study, we believe that the area involved in MERS lesions may be broader than previously recognized. That is to say, the pathology in MERS appears to extend well beyond the visible lesions.

Neonatal MERS cases have been described by Sun et al.[11] Since neonates can develop the disease even though their myelin sheaths are not yet developed, we speculate that the pathological changes in MERS are actually located in astrocytes rather than inside or beneath myelin as previously thought,[12] this is also suggested by the study of Starkey et al.[4] We further speculate that the reason for varying ADC values (cytotoxic edema) in the SCC and GCC of MERS patients is that the corpus callosum may have a special receptor or protein gradient from the posterior to the anterior. The receptor or protein most likely to be involved is aquaporin 4 (AQP4). To the best of our knowledge, no existing experiments are exactly on the gradient difference of AQP4 receptor/protein in corpus callosum. However, it is still some relevant evidence to support this speculation: Aquaporins (AQPs) are an evolutionarily conserved family of membrane transporter proteins that regulate the flow of water and in some cases, glycerol and other small molecules across cellular membranes.[13] AQP4-knockout mice show a decrease in cytotoxic brain edema after water intoxication and focal cerebral ischemia,[14] and AQP4-overexpressing mice show accelerated progression of cytotoxic brain edema.[15] These findings suggest that AQP4 contributes to the development of cytotoxic brain edema. A high concentration of AQP4 is found on astrocyte end-feet in contact with all blood vessels and astrocyte. The AQP4 distribution differs significantly within brain structures such as the hippocampus, the brainstem and particularly the corpus callosum.[16] Badaut et al.[13] reported that at high magnification, AQP4 staining in the corpus callosum reveals that AQP4 has "patchy" distribution, following the direction of the neuronal processes. This higher density leads to a tendency for the development of cytotoxic edema in the corpus callosum to develop when cytokinopathy occurs.[4] Lu et al.[17] investigated the correlations among DWI, histopathology and AQP4 expression in the rat brain that was re-perfused after acute ischemia. They found a close correlation between AQP4 expression and the cerebral intracellular edema, and that AQP4 messenger Ribonucleic acid (mRNA) expression was negatively correlated with regional ADC values. This correlation has also been reported elsewhere.[18,19] That altered ADC values may indirectly reflect the level of AQP4 expression. Various of conditions such as infection, sudden discontinuation of anti-epileptic drugs, endocrine abnormalities, and drug toxic effects, etc. which have been reported to trigger MERS, can also affect the AQP4 protein expression, leading to increased expression levels through a complex cell-cytokine[4] or an intracranial microenvironment osmotic mechanism.[20] AQP4 channel activation will result in an influx of water into astrocytes, resulting in intracellular edema and reduced diffusion (cytotoxic edema). The link between AQP4 and MERS could be indirectly tested or explained by a series of experiments and studies.[13–23] This pathogenic mechanism for MERS has not previously been proposed.

There are some limitations to our study. First, the number of subjects was relatively small. Further studies with a larger number of patients are necessary to confirm our results. Second, the body of the corpus callosum was not quantitatively measured in our study, because it is difficult to locate it in transverse diffusion imaging. However, it is much easier to locate in sagittal imaging. Therefore, sagittal DWI should be performed for MERS patients in future studies, to measure and evaluate ADC value changes and differences in all three parts of the corpus callosum (genu, body, and splenium) simultaneously. In theory, the lesion may extend to the occipital lobe (associated with the bilateral occipital forceps), the basal ganglia (associated with the corpus callosum fibers), a large portion of the parietal lobe, and even the hippocampus and the brainstem. Determining the true extent of the lesion warrants further study.

Conclusion

Our results showed that the genu of the corpus callosum shows a slight diffusion restriction in the acute stage of type I MERS, but that this recovers after treatment, as it does in the splenium of the callosum. We suggest that the lesions in type I MERS may be more widespread than previously thought. The results of this study call for further research.

Explanation of Technical Terms

READY Brain

The READY Brain protocol acquires a 3D localizer that calculates the brain center. The location of the anterior of corpus callosum (AC) and the posterior of the corpus callosum (PC) has some correlates with somewhat with the shape of the head and the anatomy of the individual patient. The system calculates the localizer for the AC–PC line from a 3D data set that is named as the Registration Localizer (READY Brain 3D Loc), which uses 3D and 2D matching technology. When Auto-Scan is added to this, it provides a one-touch protocol. READY Brain calculates the angle of the scan plane that is closest to the plane determined by the AC–PC line. Ready Brain also calculates the center of the brain, which is not necessarily the same as the mid-point of AC and PC. It is a useful tool, similar to the DOT-Brain software from Siemens Healthcare (Erlangen, Germany).

Funding

The study and collection work was funded by the Anqing Science and Technology Bureau (2018Z2018).

Conflicts of Interest

The authors declare no conflicts of interest.

References

1. Tada H, Takanashi J, Barkovich AJ, et al. Clinically mild encephalitis/encephalopathy with a reversible splenial lesion. Neurology 2004; 63:1854–1858.
2. Takanashi J. Two newly proposed infectious encephalitis/encephalopathy syndromes. Brain Dev 2009; 31:521–528.
3. Garcia-Monco JC, Cortina IE, Ferreira E, et al. Reversible splenial lesion syndrome (RESLES): what's in a name? J Neuroimaging 2011; 21:e1–e14.
4. Starkey J, Kobayashi N, Numaguchi Y, Moritani T. Cytotoxic lesions of the corpus callosum that show restricted diffusion: mechanisms, causes, and manifestations. Radiographics 2017; 37:562–576.
5. Takanashi J, Imamura A, Hayakawa F, Terada H. Differences in the time course of splenial and white matter lesions in clinically mild encephalitis/encephalopathy with a reversible splenial lesion (MERS). J Neurol Sci 2010; 292:24–27.
6. Marsala SZ, Antichi E, Pistacchi M, et al. Mild encephalitis with a reversible splenial lesion: a clinical benign condition, often underrecognized - Clinical case and literature review. J Neurosci Rural Pract 2017; 8:281–283.
7. Dardzinski BJ, Sotak CH, Fisher M, Hasegawa Y, Li L, Minematsu K. Apparent diffusion coefficient mapping of experimental focal cerebral ischemia using diffusion-weighted echo-planar imaging. Magn Reson Med 1993; 30:318–325.
8. Aksu B, Kurtcan S, Alkan A, Aralasmak A, Oktem F. Reversible corpus callosum splenial lesion due to steroid therapy. J Neuroimaging 2015; 25:501–504.
9. Lin YW, Yu CY. Reversible focal splenium lesion—MRS study of a different etiology. Acta Neurol Taiwan 2009; 18:203–206.
10. Tsubouchi Y, Itamura S, Saito Y, et al. Use of high *b* value diffusion-weighted magnetic resonance imaging in acute encephalopathy/encephalitis during childhood. Brain Dev 2018; 40:116–125.
11. Sun D, Chen WH, Baralc S, et al. Mild encephalopathy/encephalitis with a reversible splenial lesion (MERS): a report of five neonatal cases. J Huazhong Univ Sci Technol Med Sci 2017; 37:433–438.
12. Osuka S, Imai H, Ishikawa E, et al. Mild encephalitis/encephalopathy with a reversible splenial lesion: evaluation by diffusion tensor imaging. Two case reports. Neurol Med Chir (Tokyo) 2010; 50:1118–1122.
13. Badaut J, Fukuda AM, Jullienne A, Petry KG. Aquaporin and brain diseases. Biochim Biophys Acta 2014;1840: 1554–1565.
14. Ito H, Yamamoto N, Arima H, et al. Interleukin-1beta induces the expression of aquaporin-4 through a nuclear factor-kappaB pathway in rat astrocytes. J Neurochem 2006; 99:107–118.
15. Yang B, Zador Z, Verkman AS. Glial cell aquaporin-4 overexpression in transgenic mice accelerates cytotoxic brain swelling. J Biol Chem 2008; 283:15280–15286.
16. Hubbard JA, Hsu MS, Seldin MM, Binder DK. Expression of the astrocyte water channel aquaporin-4 in the mouse brain. ASN Neuro 2015; 7:pii: 1759091415605486.
17. Lu H, Hu H, He ZP. Reperfusion of the rat brain tissues following acute ischemia: the correlation among diffusion-weighted imaging, histopathology, and aquaporin-4 expression. Chin Med J 2011; 124:3148–3153.
18. Yang C, Liu Z, Li H, Zhai F, Liu J, Bian J. Aquaporin-4 knockdown ameliorates hypoxic-ischemic cerebral edema in newborn piglets. IUBMB Life 2015; 67:182–190.
19. Katada R, Nishitani Y, Honmou O, Zhai F, Liu J, Bian J. Expression of aquaporin-4 augments cytotoxic brain edema after traumatic brain injury during acute ethanol exposure. Am J Pathol 2012; 180:17–23.
20. Arima H, Yamamoto N, Sobue K, et al. Hyperosmolar mannitol stimulates expression of aquaporins 4 and 9 through a p38 mitogen-activated protein kinase-dependent pathway in rat astrocytes. J Biol Chem 2003; 278:44525–44534.
21. Ribeiro Mde C, Hirt L, Bogousslavsky J, Regli L, Badaut J. Time course of edema formation and brain aquaporin expression after transient focal cerebral ischemia in mice. J Cereb Blood Flow Metab 2005; 25:S259–S259.
22. Colbran RJ. Regulation and role of brain calcium/calmodulin-dependent protein kinase II. Neurochem Int 1992; 21:469–497.
23. Huber VJ, Tsujita M, Kwee IL, Nakada T. Inhibition of aquaporin 4 by antiepileptic drugs. Bioorg Med Chem 2009; 17:418–424.